forests

MDPI

Article

Influence of Climate and Coastal Flooding on Eastern Red Cedar Growth along a Marsh-Forest Ecotone

Sydney Hall [1], Stephanie Stotts [2,*] and LeeAnn Haaf [3]

[1] Division of Watershed Stewardship, Delaware Department of Natural Resources and Environmental Control, Dover, DE 19904, USA; sydney.hall@delaware.gov
[2] School of Agricultural and Natural Sciences, University of Maryland Eastern Shore, Princess Anne, MD 21853, USA
[3] Partnership for the Delaware Estuary, Wilmington, DE 19801, USA; lhaaf@delawareestuary.org
* Correspondence: snstotts@umes.edu

Abstract: Coastal forests in the Mid-Atlantic region are threatened by sea level rise through chronic and episodic salinization and hydrologic alterations, leading to inland marsh migration and the occurrence of ghost forests. This study uses dendrochronology to explore the impact of rising sea level on the annual growth of *Juniperus virginiana* (the Eastern red cedar) at the St. Jones component of the Delaware National Estuarine Research Reserve in Dover, DE. Chronologies from low and high elevations were developed, and a difference chronology (high–low) was generated. A rapid field assessment of tree stress indicated greater stress in low elevation trees, and low elevation soil tests showed higher soil moisture and salt content compared to samples from high elevation. Ring width indices were analyzed in relation to water level, precipitation, the Standardized Precipitation Evapotranspiration Index, and temperature, with Pearson's correlation analysis. Trees growing at low elevation showed greater climate sensitivity and responded favorably to cool, wet summers. Over time, correlations between growth and climate variables decreased, while negative correlations with tidal water level increased—a pattern that presented nearly a decade earlier in the low elevation system. Given the widespread distribution of the Eastern red cedar and its sensitivity to changes in sea level, this species may be particularly useful as a sentinel of change in coastal landscapes as sea levels rise.

Keywords: dendrochronology; sea level rise; salinization; ghost forests; forest retreat; Eastern red cedar

Citation: Hall, S.; Stotts, S.; Haaf, L. Influence of Climate and Coastal Flooding on Eastern Red Cedar Growth along a Marsh-Forest Ecotone. *Forests* **2022**, *13*, 862. https://doi.org/10.3390/f13060862

Academic Editor: Eustaquio Gil-Pelegrín

Received: 12 April 2022
Accepted: 27 May 2022
Published: 31 May 2022

1. Introduction

Coastal forests provide incredible ecosystem value, including increased biodiversity, water purification, tourism, flood protection, erosion control [1], and carbon sequestration [1,2]. These high value, low-lying coastal systems are increasingly threatened by sea level rise, which in the Mid-Atlantic averages 3–4 mm/year, with rates likely increasing to over 10 mm/year by 2100 [3,4]. Ghost forests, stands of dead trees, are becoming more widespread in the Gulf and Atlantic coasts of the United States due to the stress placed on coastal forests by sea level rise [2,5–8]. Inland migration rates, or retreat, of coastal forests in the Mid-Atlantic region are higher than other areas in the United States [6,9,10], leading to increased interest in coastal forest response to sea level rise and salinization in the region [5,11,12]. Predicting and understanding the inland migration of vulnerable and valuable coastal forests is important but difficult because forest response to sea level rise is complex and depends on both species assemblage [13] and site characteristics [6,9].

Inland forest retreat can occur gradually through chronic inundation and salinization [14,15] or through episodic events [16–18]. Young trees are often the first to die from these stressors, which is accompanied by a reduction or cessation of forest regeneration [13,19,20]. Positive feedbacks can further drive forest die-off, as increased sunlight

exposure into previously interior forests can drive surface evaporation in tandem with low tidal flushing, leaving behind excess salt [18,21,22]. Rising sea levels can also elevate the water table, causing shallow and/or asymmetric root development [23,24], which affects the mortality rate by reducing root system stability and increasing windthrow vulnerability during storm events. Climatic conditions, such as coastal storms [25], drought [13], and anthropogenic hydrologic alterations [26–28] can also create synergistic effects that influence the rate of tree mortality and retreat [13].

Annual tree growth is a result of a suite of various environmental conditions—when conditions are stressful, trees grow less. As sea level rise drives increased saltwater flooding, soil salinization causes salt accumulation within plant tissue, which can block nutrient uptake and reduce growth [29]. Dendrochronology, or the study of tree ring widths over time, can be a useful tool to study how tidal flooding and increases in flooding due to sea level rise influence tree stress in low-lying forests [5,11]. As many trees are principally influenced by climatic conditions, analyzing tree ring widths relative to tidal water level, in combination with temperature, precipitation, and/or drought, elucidates key relationships that influence the variability of tree mortality and therefore forest retreat, as sea levels rise.

Dendrochronology is an important tool that has provided valuable insights regarding tree response to salinization [5,11]. However, the relationship between annual tree growth and visible expressions of tree stress are not yet well understood, which hinders our understanding of the processes that drive coastal forest retreat. Questions remain about mechanisms of forest retreat with sea level, such as *does tree growth decline before or after salt accumulates in the soil?* In addition, *are low elevation trees experiencing more stress than higher elevation trees due to differences in soil chemical composition?* This study seeks to provide a more complete understanding of the processes involved in coastal forest retreat, by adding in situ rapid tree stress assessment and soil chemical analyses to traditional dendrochronology, at a site already experiencing changes relative to rising sea level.

In addition to using a novel approach of rapid tree stress assessment and soil chemical analyses to study mechanisms of coastal forest retreat, this study also seeks to expand dendrochronological analysis to an important but understudied coastal forest species, the Eastern red cedar (*Juniperus virginiana* L. var. *virginiana*). The Eastern red cedar occurs throughout the eastern United States as a common component of early to mid-successional forests and is also one of the most salt tolerant tree species found in these temperate forests [13,20]. Eastern red cedars frequently occupy low-lying maritime or coastal forests throughout their range. While greenhouse studies have examined the impact of salinization and inundation on the Eastern red cedar [30], a dendrochronological study of this species in a sea-level rise impacted system has not yet been published. Therefore, this study explores how differences in flooding influences Eastern red cedar growth patterns along an elevation gradient at the St. Jones Reserve in Dover, Delaware, using dendrochronology, in situ rapid tree stress assessment methods, and soil chemical analyses.

2. Materials and Methods

2.1. Study Species

The Eastern red cedar is ubiquitous in the eastern United States. This widely distributed species can be found in every state east of the 100th meridian, ranging from Texas to Southern Ontario and extending well into the great plains [31]. As a shade intolerant, pioneering species [32], the Eastern red cedar is known for its ability to survive extreme environmental conditions, including temperatures ranging from −29 °C to 41 °C, as little as 38.1 cm of precipitation during the growing season, elevations from sea level to 1500 m, and varying soil types from deep and shallow soils to thin and rocky soils [33]. Exhibiting moderate salinity tolerance, Eastern red cedars are commonly found growing on barrier islands [34], swales [20,35], and dunes [36], and have been reported to survive salinities up to 1400 ug/g [30].

2.2. Study Site

Samples were collected from both the St. Jones Reserve and the Ted Harvey Wildlife Area in Dover, Delaware (Figure 1). The St. Jones Reserve is managed by the Delaware National Estuarine Research Reserve (DNERR) in the Delaware Department of Natural Resources and Environmental Control. The Ted Harvey Wildlife area is located 2.5 km downstream from the DNERR and is managed by Delaware Fish and Wildlife. Due to proximity, the conditions at the Ted Harvey Wildlife Area were assumed to be the same as those at the St. Jones Reserve.

Delaware has a temperate climate; summers are hot with an average temperature of 23.0 °C, while the winters average about 3.2 °C [37]. Precipitation varies seasonally, with an average sum of 32.4 cm in summer months and an average sum of 26.5 cm in the winter. Tropical storms and hurricanes impact this area most often between the months of August and October. Although Delaware is less susceptible to a direct hit from these larger storm events, extra tropical coastal storms can cause severe coastal floods [38].

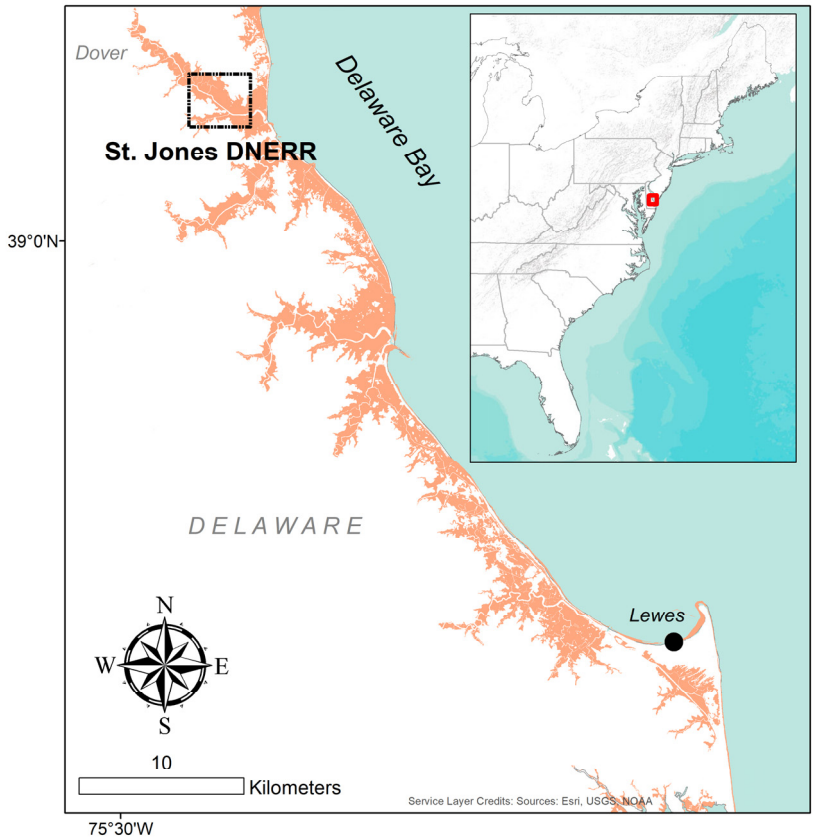

Figure 1. Map of study site at the St. Jones DNERR in Kent County, DE (black box), with orange fill indicating the location of tidal marshes. Water level in this study was obtained from the Lewes NOAA tide gauge (black dot). The inset shows the position of the study site within the Mid-Atlantic, along the East Coast of the U.S., with the map extent indicated by a red box.

2.3. Field Methods

The locations of saplings (diameter at breast height <10 cm) within the study site were surveyed with a handheld GPS unit in winter to reduce interference from deciduous trees in the canopy. The locations of these trees were then plotted in GIS and combined with LiDAR data to identify the land surface elevation associated with the lack of tree regeneration, establishing the division between high and low forest. Accuracy of the LiDAR is reported to have met Quality Level 2 requirements, with an open terrain accuracy of 6.3 cm, with slight errors in heavily vegetated areas [39].

After the boundary between high and low elevation was established, a rapid assessment of tree stress was performed to compare tree stress between these elevation categories. Existing rapid field assessments focus on the ecosystem [40] or the ecological and economic impacts of trees on the environment [41] and were too broad for this study. Therefore, a rapid assessment to quantify tree stress was developed from existing assessments. The assessment in this study included indicators of stress such as small or wilted needles, dead or missing limbs, tipping, flaking and discolored bark [42], foliage color, branches distribution, and tree regeneration [43]. Individual trees were evaluated for 19 indicators of stress and were assigned a score between zero and 4 based on visual assessment, with zero indicating the greatest expression of stress (Table S1). The total score was divided by 76, the highest potential score, resulting in a score percentage with low values indicative of greater stress. The assessment was conducted on 48 trees selected to represent a range of elevations from the marsh edge to the upland boundary.

Tree ring samples were collected with a Haglöf 5 mm increment borer. Individual tree selection was based on size (>15 cm diameter at breast height) and overall condition (e.g., free of obvious damage, rot, or disease). The Eastern red cedar infrequently occurs above the high elevation line (1.2 m) within the St. Jones Reserve, so a comprehensive sample of 36 trees were cored in duplicate beyond the central pith. Samples from 23 low elevation trees were collected. Post collection, each sample was air dried for 24 h before being glued into wooden mounts. After drying to ensure stability within the mounts, each core was then sanded with progressively finer sandpaper (220 to at least 800 coarseness). Tree rings were counted and measured using a Velmex Unislide linear encoder (Velmex, Inc., Bloomfield, NY, USA) and MeasureJ2X software (VoorTech Consulting, Holderness, NH, USA) with 0.001 mm precision.

2.4. Laboratory Methods

The high and low elevation soil was tested by the University of Delaware's Core Laboratory for Soil, Plant and Water Analysis. The soil was tested for water pH, A-E buffer pH, organic matter by loss on ignition, M3-P, K, Ca, Mg, Mn, Zn, Cu, Fe, Na, S, B, Al, cation exchange capacity (CEC), percent base saturation (%BS), threshold phosphorus saturation ratio (PSR), and soluble salts. Soil property characterizations were also tested for moisture content and water pH, along with nitrate and ammonium–nitrogen by 2M KCl extraction. Eight soil samples were collected to a depth of 10–20 cm in at least 5 cm slices, cleaning the spade between every collection, following the University of Delaware Soil Testing Program's protocol [44]. Four samples in both the high and the low areas were selected at random using grids and a random number generator.

For tree ring chronologies, the list method was initially used to determine any marker rings or anomalies to cross-date between the series for the chronologies [45]. Cross-dating verification was performed with COFECHA [46]. The Eastern red cedar at this site produces eccentric lobular growth, which can produce highly irregular growth rings depending on the sampling path. Rings that could not be reliably recognized were omitted from the study. The chronology from the low elevation site was constructed from 14 trees and the chronology from the high elevation site was constructed from 13 trees. A master chronology was also constructed from all the trees included in the chronologies from high and low elevation. Individual chronologies were detrended using 50% frequency cutoff two thirds splines for conversion to ring width indices (RWI). We used biweight robust means to create mean chronologies (i.e., master, high elevation trees, and low elevation trees) in R statistical software with the "dplR" package [47]. To reduce autoregressive structures and transient disturbances, we prewhitened these chronologies for climatic and water level correlations [48]. A chronology of the differences between high and low elevation tree growth was created by subtracting the mean chronology of low elevation trees from the mean chronology of high elevation trees [11]. The standardization was run on a per-tree basis as a means to reduce deterministic patterns related to geometric tree growth. Using RWI therefore removes age-specific differences, producing the annual age-standardized

average growth across all trees. Therefore, the difference chronology represents the age-standardized mean growth differences between the high and low elevation trees.

2.5. Data Analysis

The mean stress percentage was computed for both the high and low elevation study areas. An unpaired independent *t*-test for two samples assuming unequal variances was performed to compare the high and low soil and tree stress data (*p*-value significance for one tail 0.05 > at 95% CI). For soil data, tests were performed on each nutrient parameter.

Temperature and precipitation data were obtained from the National Centers for Environmental Information (NCEI) regional climate datasets. For drought, we used the Standardized Precipitation Evapotranspiration Index (SPEI) from the Climate Engine [49]. Maximum monthly water levels were obtained from the Lewes, DE, National Oceanic and Atmospheric Administration (NOAA) real-time gauge (station #8557380; [50]). The Lewes tide gauge is 42 km from the study site, but the tide gauge maintained at the DNERR was short (ca. 2008). In a previous analysis, the Lewes tide gauge was a suitable proxy to explore relationships with tidal water levels at the DNERR [11]. Before 1980, NOAA monthly water level records were irregular at the Lewes gauge, with many missing monthly values; therefore, correlation analyses were run from 1980 to 2019.

We ran Pearson's correlation tests on the RWI, temperature anomalies (1901–2000 base period), precipitation anomalies (1901–2000 base period), drought (SPEI), and maximum tidal water levels, similar to Haaf et al. [11]. Correlation tests were performed monthly from the antecedent June to the concurrent September for all climate and water level data. Partial correlation tests of these variables were carried out using 95% confidence intervals to determine the significance of each test, similar to Haaf et al. [11]. Partial correlation tests were performed monthly from the antecedent August to the concurrent September.

As growth relationships with rising sea levels might be non-stationary, moving response functions (MRF) were run on temperature and drought partial correlation tests with seasonal water level data to assess variability over time [50,51]. MRFs assessed correlations over an abbreviated time window (n = 24 years) and reassessed the correlation after sliding the window one year forward. Environmental variables were summarized by season, where January–March is winter, April–June is spring, July–September is summer, and October–December is autumn. Temperature and the SPEI were summarized by the seasonal means, whereas water level and precipitation were summarized by seasonal sums. We chose to use water level sums because higher water level was a proxy for flood exposure, which is likely more similar to precipitation in that it could have a cumulative effect on moisture availability or salt accumulation. MRFs between seasonal water levels and RWI were evaluated for change over time through generalized least square linear regression with autoregressive error ($\alpha = 0.05$).

3. Results

GPS surveys at the study site combined with LiDAR data did not show any tree regeneration below 1.2 m (4 feet) relative to the North American Vertical Datum of 1988 (NAVD88). Based on these results, the 1.2 m elevation contour delineated low from high elevation forest. Trees growing at less than 1.2 m elevation had a mean stress score of 38.09 ($\pm$10.33) percent, while trees growing above this elevation had a mean stress score of 76.22 ($\pm$14.85) ($p < 0.001$). The forested buffer is narrow at the study site ranging from 20 to 150 m wide.

Soil analysis results show that the low elevation soil samples had higher mean values of 90.5 mg/kg for K ($p = 0.017$), 491.5 mg/kg for Mg ($p = 0.009$), 762.2 mg/kg for Na ($p < 0.001$), 61.6 mg/kg for Fe ($p < 0.001$), 14.87 mg/kg for S ($p = 0.009$), 1.45 mg/kg for B ($p = 0.0033$), 5.37 meq/100 g for CEC ($p = 0.018$), 0.625 mmhos/cm higher for soluble salts ($p = 0.005$), 49.55% for OM ($p = 0.001$), and 24.38 mg/kg for ammonium nitrogen ($p = 0.002$) than the high elevation samples. The high elevation samples had a higher mean value of 415.2 mg/kg of Al ($p < 0.001$) than the low elevation samples. No significant differences

were found between the high and low elevation means for P, Mn, Zn, Ca, Cu, P sat. ratio, A-E buffer pH, nitrate, or water pH (Table S2).

The master chronology included 27 trees with an interseries correlation of 0.434 and a mean sensitivity, a statistic indicative of stand responsiveness to climate [52], of 0.328. A total of 8 missing rings were detected in high elevation trees only: 1991 (n = 2), 1993 (n = 1), 2007 (n = 4), and 2011 (n = 1). The chronology from high elevation included 13 trees with an interseries correlation of 0.402 and a mean sensitivity of 0.350 (Data S1). The ages of the trees in this chronology ranged from 14 to 79 years, with an average age of 45.4 years. The chronology from low elevation included 14 trees with an interseries correlation of 0.475 and a mean sensitivity of 0.307 (Data S2). Trees in this chronology ranged from 16 to 52 years, with an average age of 42.5 years (Figure 2). The diameter at breast height did not differ between the high and low groupings.

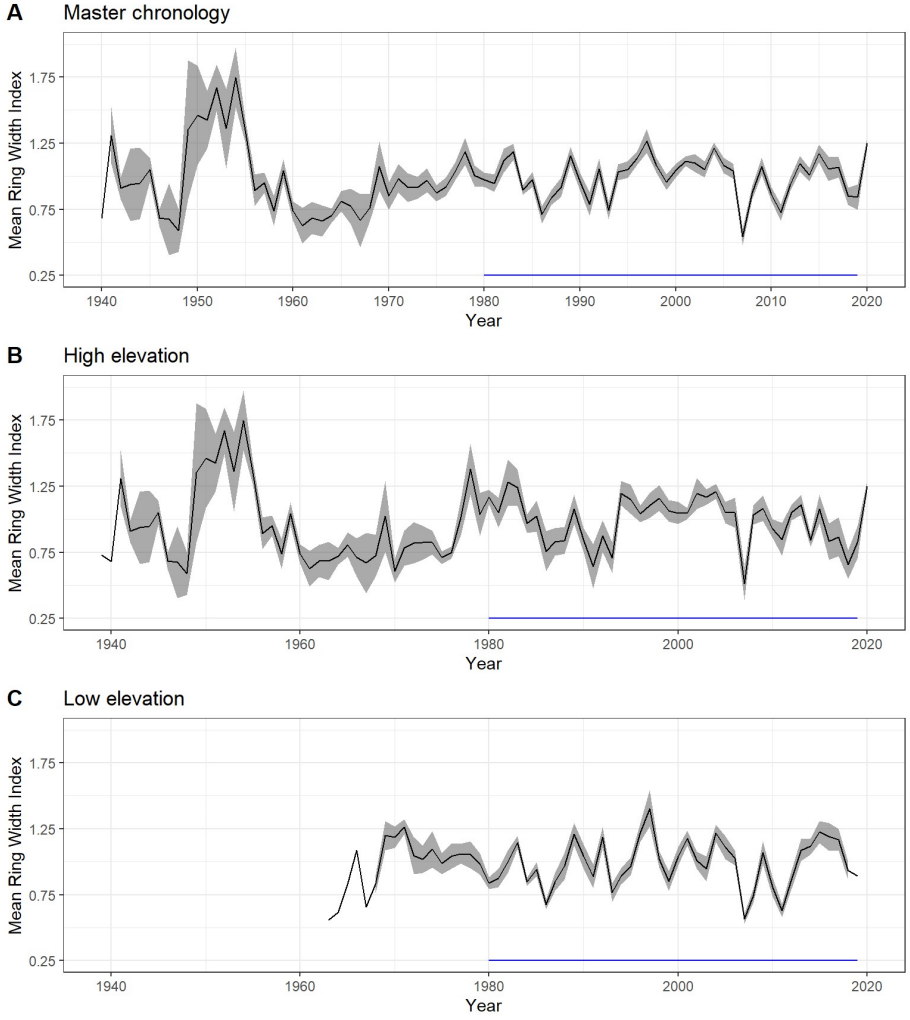

Figure 2. Mean chronologies for (**A**) the master chronology including all trees, (**B**) the chronology including specimens growing at elevations greater than 1.2 m relative to NAVD88, (**C**) the chronology including specimens growing at elevations lower than 1.2 m relative to NAVD88. The mean chronologies (black line) are bound by standard error (grey ribbon) with a horizontal blue line indicating the length of the environmental records (water level, specifically) used for correlation analyses, which was 1980–2019.

The master chronology was significantly ($p < 0.05$) and positively correlated with June precipitation (R = 0.479) and the June SPEI (R = 0.330). When included in a partial correlation analysis with precipitation (R = −0.325), the SPEI (R = −0.325), or water level (R = −0.325), June temperature was negatively correlated with tree growth. The positive

correlation between the SPEI and growth also expanded into July (R = 0.391). When analyzed over the duration of the chronology, the strong positive correlation between both June precipitation and the SPEI with RWI weakened and even lost significance, while the negative correlation between water level increased.

When analyzed separately, the chronology from low elevation was positively correlated with June precipitation (R = 0.479) and the June through August SPEI (0.244 < R < 0.306). The partial correlation results, including temperature and water level, indicated significant negative correlations between temperature and RWI for June (R = −0.378) and July (R = −0.401), and negative correlations between water level and growth for April (R = −0.410) and May (R = −0.280; Figure 3). The strength of the correlation for the SPEI decreases over time, remaining significant over the duration of the analysis for precipitation but losing significance for the SPEI in the early 1990s. The correlation between RWI and growing season (April–June) water level was significantly negatively correlated in the mid-1980s, with the strength of the correlation increasing over time (Figure 4).

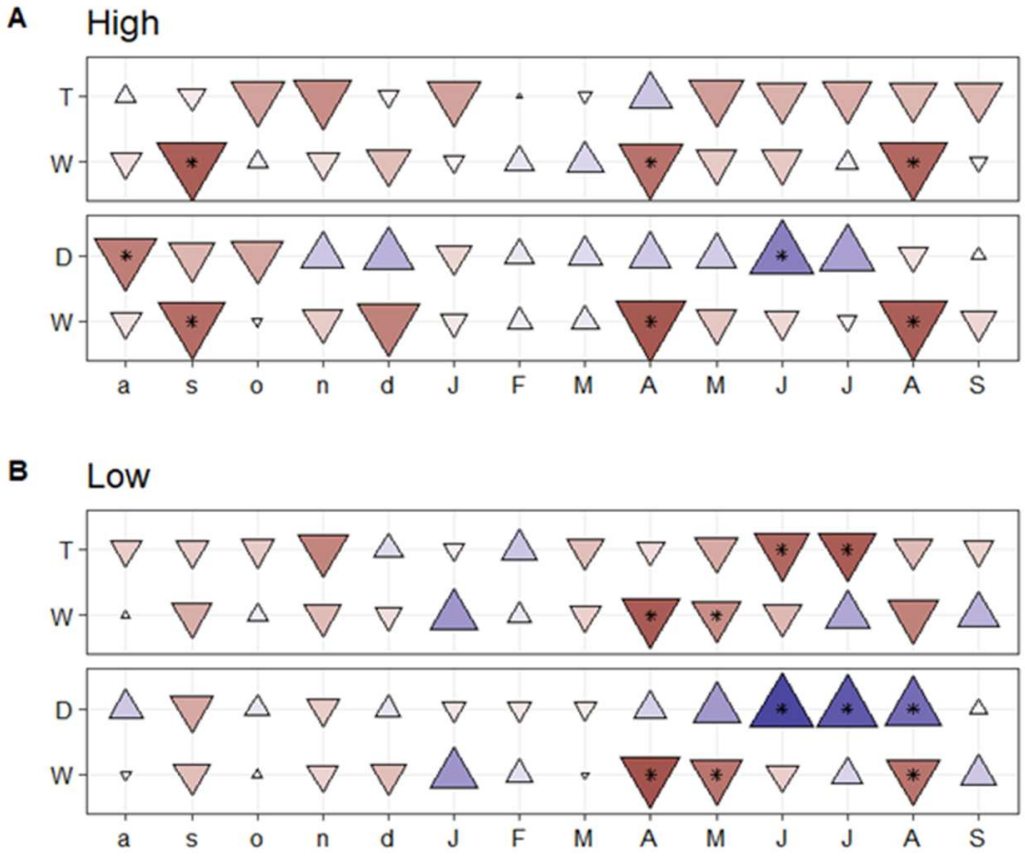

Figure 3. Partial correlation results for (**A**) the chronology from high elevation and (**B**) the chronology from low elevation. Pairwise tests consisting of temperature (T) or SPEI/Drought (D) and water level (W). Upwards, blue triangles represent positive correlations, whereas negative correlations are represented by downwards, red triangles. Symbol saturation and size are strength of the correlation (i.e., R), ranging from +0.5 to −0.5. Significant correlations are noted with an asterisk ($p < 0.05$). Antecedent months are lower-case letters, whereas concurrent months are capital letters.

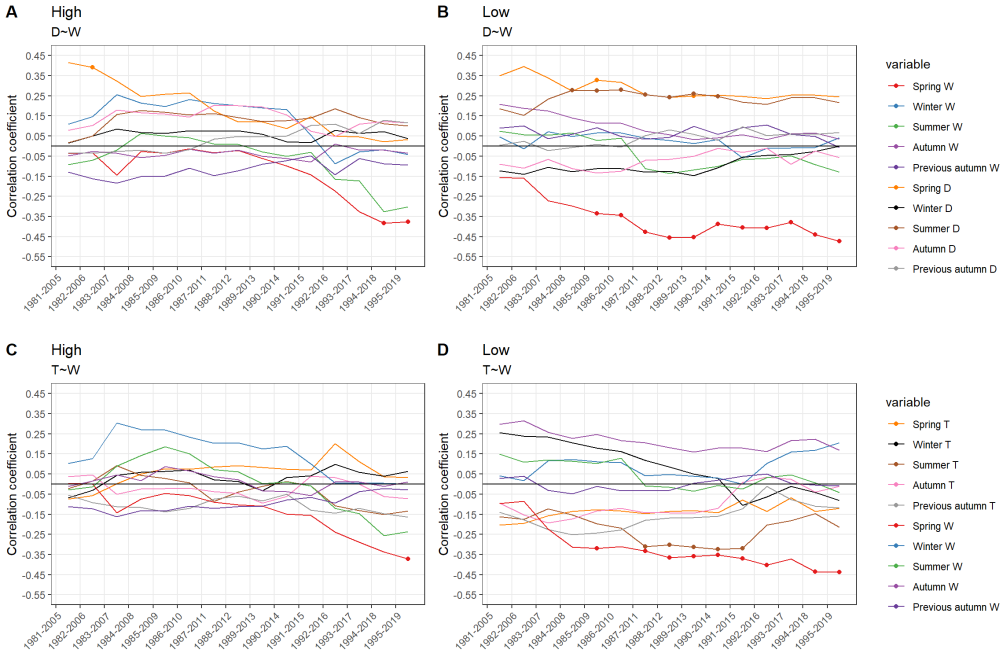

Figure 4. Moving response function of Pearson's correlation analysis using a 24-year window results for (**A**) RWI from high elevation and SPEI/Drought (D) and water level (W), (**B**) RWI from low elevation and SPEI/Drought (D) and water level (W), (**C**) RWI from high elevation and temperature (T) and water level (W), and (**D**) low elevation RWI and temperature (T) and water level (W). The trace plots lines are seasonal groupings of temperature or drought and water level for winter (January–March), spring (April–June), summer (June–September), autumn (October–December), and previous autumn. Significant correlations are noted with solid dots ($p < 0.05$).

For the chronology from high elevation, June precipitation was positively correlated to growth (R = 0.325) but lost statistical significance in the late 1980s. Significant positive correlations were found in April (R = 0.280) between temperature and RWI, while positive correlations were found for water level in the previous June (R = 0.222). Partial correlation analysis for the chronology from high elevation, including temperature and water level, produced negative correlations between water level and RWI for the previous September (R = −0.362) and the concurrent April (R = −0.349) and August (R = −0.378). The correlation for the SPEI also diminished over the study period, losing significance in the early 1980s. The correlation between RWI and water level remained very low for this chronology over much of the study period, but rapidly developed negative correlation coefficients in the early 1990s, becoming statistically significant in the mid-1990s (Figure 4).

The RWI differences produced positive values in 26 of the study years, indicating conditions favoring growth for trees at high elevation, while negative values, indicating favorable growth conditions for trees growing at low elevation, occurred in 31 of the study years (Figure 5). Partial correlation analysis between the difference chronology and water level showed significant negative correlation between the difference index and January water levels when combined with either the SPEI or temperature. When analyzed with water level, the SPEI produced significant negative correlations with the difference index for the previous August and October and the current August (Figure 6).

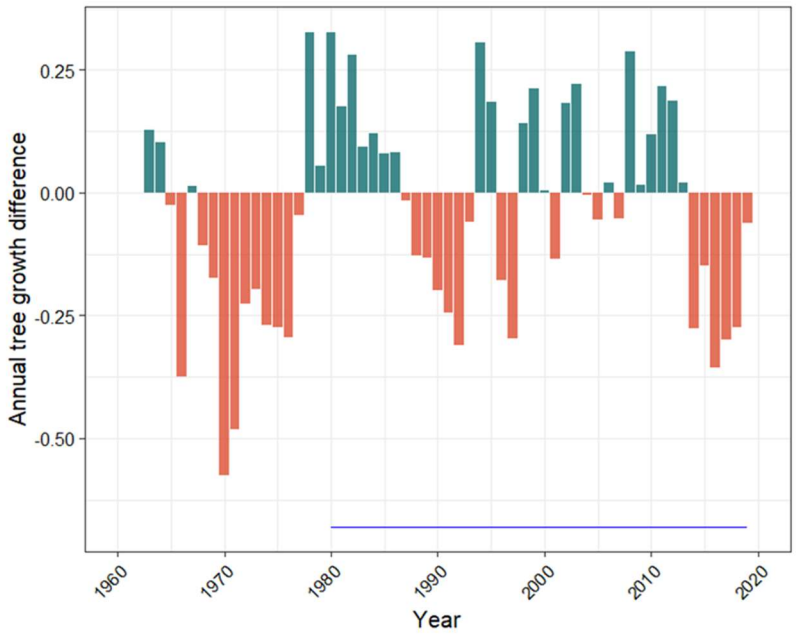

Figure 5. A chronology of the RWI difference between high and low elevation trees. Green represents positive differences, indicating conditions favoring growth in trees at high elevation and orange represents negative differences, indicating conditions favoring growth in trees at low elevations. The blue horizontal line shows the period from 1980–2019, which is the extent of the water level records.

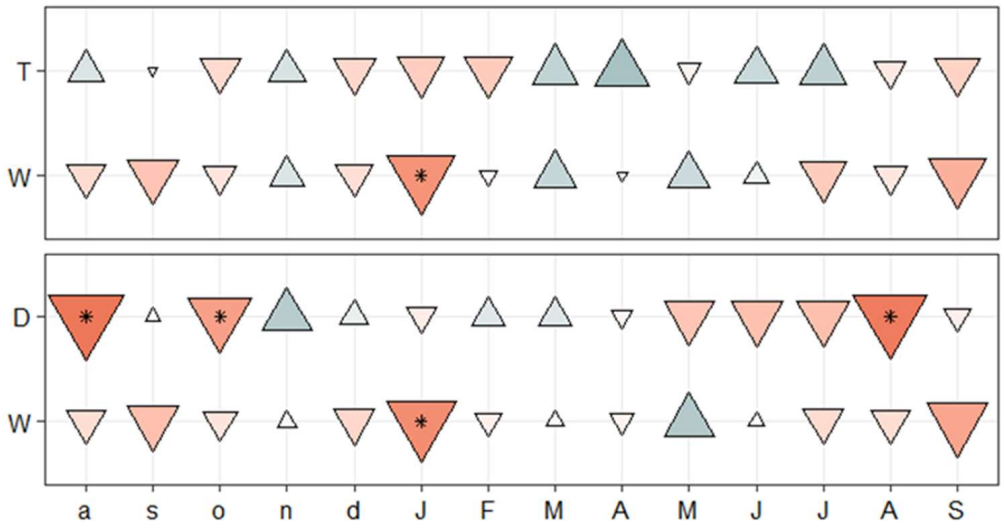

Figure 6. Partial correlation results for mean growth difference between high and low elevation trees. Pairwise tests were temperature (T) or SPEI/drought (D) and water levels (W). Positive correlations (upwards, green triangles) show correlation relationships where high elevation tree growth means were larger than low elevation trees, whereas negative correlations (downwards, orange triangles) are where growth means for low elevation trees were larger than means for high elevation trees. The saturation and size of symbols reflect correlation strength (i.e., R from +0.5 to −0.5). Significant correlations are noted with an asterisk ($p < 0.05$). Antecedent months are lower-case letters, whereas concurrent months are capital letters.

4. Discussion

This study combined in situ rapid tree stress assessment methods and soil chemical analyses with dendrochronology, to provide a more complete understanding of the processes and mechanisms involved in coastal forest retreat at the St. Jones Reserve in Dover, DE, a system impacted by sea level rise.

4.1. Flooding and Subsequent Stress along an Elevation Gradient

To explore flooding and subsequent stress along an elevation gradient, tree stress scores and soil parameters were compared between high and low elevation forest. The rapid assessment of tree stress confirmed the 1.2 m contour as the delineation line between high and low forest, showing significantly more stress in the low elevation trees compared to those in the high elevation. Haaf et al. [11] delineated high and low forest at the St. Jones DNERR using quantitative methods, based on threshold flood levels set using water level data and digital elevation models (DEM), establishing the 1.0 m contour as the boundary between high and low elevation forest. The selection of the 1.2 m contour in this study supports the results of Haaf et al. [11], finding a similar delineation based on habitat characteristics. None of the trees included in this study were growing between 1.0 and 1.2 m in elevation.

The results of soil testing also support the hypothesis that flooding produces stress to trees growing at low elevation, as soil samples collected below 1.2 m had significantly greater quantities of soluble salts and elements typically associated with salinization, including boron, sodium, potassium, and magnesium. Tallie et al. [7] also found elevated concentrations of cations in salinized soil and used sodium as a proxy for saltwater exposure, finding sodium content to be a better predictor of vegetation change than land surface elevation. Furthermore, some elemental concentrations in the low elevation study area were beyond toxicity thresholds. For example, boron is toxic to trees at levels above 0.5 to 1.0 $mg \cdot kg^{-1}$ [53] and is found in concentrations of 2.128 $mg \cdot kg^{-1}$ in the low elevation study site but within range in high elevation soils.

4.2. Growth Response of Eastern Red Cedar along an Elevation Gradient

The use of the Eastern red cedar in dendrochronology can be problematic as this species is prone to false rings [54–57]. In addition to false rings, irregular growth patterns made some cores impossible to interpret. Despite these shortcomings, the Eastern red cedar was selected for this study because it is the most widespread native conifer in Eastern North America [31] and exhibits moderate salt tolerance [30].

Trees growing at low and high elevation in this study displayed different climate sensitivities, in terms of the number of months with significant correlations and the strength of the correlation coefficients. Eastern red cedar growth is typically correlated with low summer temperatures, high summer precipitation, and high summer drought indices [56,58,59]—trends which were also present in this study (Figure 3). However, the chronology from high elevation only displayed significant correlations between June ($R = 0.343$) and the previous August SPEI ($R = -0.319$), whereas the chronology from low elevation was significantly correlated with low temperatures in June ($R = -0.378$) and July ($R = -0.407$) and a high SPEI in June, July, and August ($0.398 < R < 0.510$). Differences in saltwater flood exposure is a likely mechanism of this climate sensitivity divergence, a hypothesis that is also supported by differences in soil chemical composition.

The impact of sea level rise on growth response in coastal trees was examined using tidal water level, a variable not included in other published studies of the Eastern red cedar. Partial correlation analysis results indicate that water level is an important driver of annual tree growth with significant negative correlations occurring between both the chronologies from high and low elevation and the water level for April and August. The duration of the correlation extends into May for the low elevation analysis and is found in the previous September in the high elevation analysis (Figure 3). These results support other studies indicating that sea level, and therefore flood exposure, are important controls of growth in coastal forest systems [11,60], and that these effects may extend beyond the range of tidal influence [60].

According to the moving response function analysis, the drivers of growth in the Eastern red cedar varied over time and differed between elevation classes, with the high elevation response lagging behind the low elevation by approximately 10 years. The negative correlation between spring water level and RWI for low elevation trees, rapidly

increased in strength, becoming statistically significant as the window of analysis shifted from 1982 to 1986 (Figure 4). Spring water level then became the dominant driver of growth as correlations with climatic variables weakened and lost statistical significance, while the correlations with water level became increasingly negative. The same trends appear in the high elevation trees as the correlation between RWI and spring water level hovered around zero for study windows starting in 1981–1991. Then, correlation coefficients became increasingly negative, reaching statistical significance by 1994. These results are important because they indicate that tree growth response to rising sea level can occur rapidly, before visible signs of stress become apparent. These temporal thresholds will likely be important for predicting changes in forest vulnerability to stress and retreat.

This study did not include channel water salinity in the correlation analysis due to data availability, but increased salinity has been known to cause decreased annual growth [29,61,62]. Although counterintuitive, pulses of salinity have also been correlated to increased annual growth in the initial stages of salinization [60], leading researchers to hypothesize that surviving trees may benefit from reduced competition [63] and enhanced primary productivity [64], due to increased inorganic N and P availability [65,66] in the early stages of salinization. This hypothesis might also explain why the lower elevation trees in this study did not consistently grow less compared to high elevation trees on average (Figures 5 and 6). Lower elevation trees in this study, however, showed greater visible signs of stress, including fewer limbs and needles. Fewer needles would demand less water and nutrients, and this could make low elevation trees more resistant to pulse disturbances, such as storm surge or windthrow events, than their fuller counterparts at higher elevations.

5. Conclusions

The growth response of the Eastern red cedar to flooding and subsequent stress along an elevation gradient was explored with dendrochronology, rapid tree stress assessment, and soil samples. Trees growing at low elevation (<1.2 m NAVD88) had greater stress scores based on visible signs of stress, including small or wilted needles, dead or missing limbs, tipping, flaking and discolored bark, and foliage discoloration, than their higher elevation counterparts. Low elevation soil had more soluble salts, potassium, magnesium, sodium, iron, sulfur, boron, cation exchange capacity, organic matter, and ammonium nitrogen, with some parameters above the toxicity threshold. Trees at both elevations displayed climate growth relationships typical for the species, including favorable responses to cool, wet summers, but climate sensitivity was higher in low elevation trees. High tidal water levels in the spring and fall were associated with reduced annual growth, regardless of elevation. Early in the chronologies, tidal water level had little effect on tree growth. However, as the sea level rose, the water level became increasingly correlated to reduced annual growth, eventually becoming a more significant driver of growth than climate. This shift in the importance of water level as a driver of growth in the high elevation forest lagged approximately 10 years behind the low elevation forest, with growth responses occurring ahead of visible signs of stress and changes in soil composition. Despite obvious signs of stress and forest decline in the low elevation forest, Eastern red cedars often outperformed their higher elevation counterparts, particularly in years following wet falls. In a salinizing system, the Eastern red cedar may benefit from reduced competition under favorable conditions. This study indicates that shifts in drivers of growth in the Eastern red cedar—a hardy and widespread species—from climate to tidal water level may serve as sentinels of change in coastal landscapes as climates change and sea levels rise.

Supplementary Materials: The following supporting information can be downloaded at: https://www.mdpi.com/article/10.3390/f13060862/s1, Table S1: Rapid stress assessment example; Table S2: Soil sample results; Data S1: High Elevation Tree Ring Measurements.csv; Data S2: Low Elevation Tree Ring Measurements.csv.

Author Contributions: Conceptualization, methods, S.S. and S.H.; data collection, S.H.; formal analysis, L.H.; draft preparation, S.S.; review and editing, S.S., S.H. and L.H.; funding acquisition, S.S. All authors have read and agreed to the published version of the manuscript.

Funding: This publication (or program) was made possible by the National Science Foundation Critical Zone Network Cluster Grant No. 2012484, the National Science Foundation Delaware EPSCoR (Established Program to Stimulate Competitive Research) grant number OIA-1757353, and the Delaware Space Grant College and Fellowship Program, NASA Grant 80NSSC20M0045.

Data Availability Statement: Publicly available data used in this study can be found at the hyperlinks provided within the references list, which includes data from the NOAA and USGS. Ring width, and soil and tree stress measurements are included in the supplementary materials.

Acknowledgments: The authors are grateful for the support of Joseph Howard and Kassandra Rodriguez for help with data collection and the Delaware National Estuarine Research Reserve (Kari St. Laurent and Robert Hossler) for field site access.

Conflicts of Interest: The authors declare no conflict of interest.

References

1. Barbier, E.B.; Hacker, S.D.; Kennedy, C.; Koch, E.W.; Stier, A.C.; Silliman, B.R. The Value of Estuarine and Coastal Ecosystem Services. *Ecol. Monogr.* **2011**, *81*, 169–193. [CrossRef]
2. Smart, L.S.; Taillie, P.J.; Poulter, B.; Vukomanovic, J.; Singh, K.K.; Swenson, J.J.; Mitasova, H.; Smith, J.W.; Meentemeyer, R.K. Aboveground Carbon Loss Associated with the Spread of Ghost Forests as Sea Levels Rise. *Environ. Res. Lett.* **2020**, *15*, 104028. [CrossRef]
3. Kopp, R.E.; Andrews, C.J.; Garner, A.; Miller, J.A.; Broccoli, A.; Kreeger, D.; Miller, J.K.; Leichenko, R.; Lin, N.; Little, C.M.; et al. *New Jersey's Rising Seas and Changing Coastal Storms: Report of the 2019 Science and Technical Advisory Panel*; Rutgers: New Brunswick, NJ, USA, 2019.
4. Callahan, J.A.; Horton, B.P.; Nikitina, D.L.; Sommerfield, C.K.; McKenna, T.E.; Swallow, D. *Recommendation of Sea-Level Rise Planning Scenarios for Delaware: Technical Report, Prepared for Delaware Department of Natural Resources and Environmental Control (DNREC) Delaware Coastal Programs*; Delaware Geological Survey: Newark, DE, USA, 2017.
5. Kirwan, M.L.; Kirwan, J.L.; Copenheaver, C.A. Dynamics of an Estuarine Forest and Its Response to Rising Sea Level. *J. Coast. Res.* **2007**, *232*, 457–463. [CrossRef]
6. Schieder, N.W.; Walters, D.C.; Kirwan, M.L. Massive Upland to Wetland Conversion Compensated for Historical Marsh Loss in Chesapeake Bay, USA. *Estuaries Coasts* **2018**, *41*, 940–951. [CrossRef]
7. Taillie, P.J.; Moorman, C.E.; Poulter, B.; Ardón, M.; Emanuel, R.E. Decadal-Scale Vegetation Change Driven by Salinity at Leading Edge of Rising Sea Level. *Ecosystems* **2019**, *22*, 1918–1930. [CrossRef]
8. Schieder, N.W.; Kirwan, M.L. Sea-Level Driven Acceleration in Coastal Forest Retreat. *Geology* **2019**, *47*, 1151–1155. [CrossRef]
9. Smith, J.A.M. The Role of Phragmites Australis in Mediating Inland Salt Marsh Migration in a Mid-Atlantic Estuary. *PLoS ONE* **2013**, *8*, e65091. [CrossRef]
10. Hussein, A.H. Modeling of Sea-Level Rise and Deforestation in Submerging Coastal Ultisols of Chesapeake Bay. *Soil Sci. Soc. Am. J.* **2009**, *73*, 185–196. [CrossRef]
11. Haaf, L.; Dymond, S.F.; Kreeger, D.A. Principal Factors Influencing Tree Growth in Low-Lying Mid Atlantic Coastal Forests. *Forests* **2021**, *12*, 1351. [CrossRef]
12. Kirwan, M.L.; Gedan, K.B. Sea-Level Driven Land Conversion and the Formation of Ghost Forests. *Nat. Clim. Chang.* **2019**, *9*, 450–457. [CrossRef]
13. Desantis, L.R.G.; Bhotika, S.; Williams, K.; Putz, F.E. Sea-Level Rise and Drought Interactions Accelerate Forest Decline on the Gulf Coast of Florida, USA. *Glob. Change Biol.* **2007**, *13*, 2349–2360. [CrossRef]
14. Mulholland, P.J.; Best, G.R.; Coutant, C.C.; Hornberger, G.M.; Meyer, J.L.; Robinson, P.J.; Stenberg, J.R.; Turner, R.E.; Vera-Herrera, F.; Wetzel, R.G. Effects of Climate Change on Freshwater Ecosystems of the South-Eastern United States and the Gulf Coast of Mexico. *Hydrol. Processes* **1997**, *11*, 949–970. [CrossRef]
15. Herbert, E.R.; Boon, P.; Burgin, A.J.; Neubauer, S.C.; Franklin, R.B.; Ardón, M.; Hopfensperger, K.N.; Lamers, L.P.M.; Gell, P. A Global Perspective on Wetland Salinization: Ecological Consequences of a Growing Threat to Freshwater Wetlands. *Ecosphere* **2015**, *6*, art206. [CrossRef]
16. Chapman, E.L.; Chambers, J.Q.; Ribbeck, K.F.; Baker, D.B.; Tobler, M.A.; Zeng, H.; White, D.A. Hurricane Katrina Impacts on Forest Trees of Louisiana's Pearl River Basin. *For. Ecol. Manag.* **2008**, *256*, 883–889. [CrossRef]
17. Middleton, B.A. Differences in Impacts of Hurricane Sandy on Freshwater Swamps on the Delmarva Peninsula, Mid-Atlantic Coast, USA. *Ecol. Eng.* **2016**, *87*, 62–70. [CrossRef]
18. Fagherazzi, S.; Anisfeld, S.C.; Blum, L.K.; Long, E.V.; Feagin, R.A.; Fernandes, A.; Kearney, W.S.; Williams, K. Sea Level Rise and the Dynamics of the Marsh-Upland Boundary. *Front. Environ. Sci.* **2019**, *7*, 25. [CrossRef]

19. Brinson, M.M.; Christian, R.R.; Blum, L.K. Multiple States in the Sea-Level Induced Transition from Terrestrial Forest to Estuary. *Estuaries* **1995**, *18*, 648–659. [CrossRef]
20. Williams, K.; Meads, M.V.; Sauerbrey, D.A. The Roles of Seedling Salt Tolerance and Resprouting in Forest Zonation on Thewest Coast of Florida, USA. *Am. J. Bot.* **1998**, *85*, 1745–1752. [CrossRef]
21. Wendelberger, K.S.; Richards, J.H. Halophytes Can Salinize Soil When Competing with Glycophytes, Intensifying Effects of Sea Level Rise in Coastal Communities. *Oecologia* **2017**, *184*, 729–737. [CrossRef]
22. Williams, K.; Ewel, K.C.; Stumpf, R.P.; Putz, F.E.; Workman, T.W. Sea-Level Rise and Coastal Forest Retreat on the West Coast of Florida, Usa. *Ecology* **1999**, *80*, 2045–2063. [CrossRef]
23. Fan, Y.; Miguez-Macho, G.; Jobbágy, E.G.; Jackson, R.B.; Otero-Casal, C. Hydrologic Regulation of Plant Rooting Depth. *Proc. Natl. Acad. Sci. USA* **2017**, *114*, 10572–10577. [CrossRef] [PubMed]
24. Messerschmidt, T.C.; Langston, A.K.; Kirwan, M.L. Asymmetric Root Distributions Reveal Press–Pulse Responses in Retreating Coastal Forests. *Ecology* **2021**, *102*, e03468. [CrossRef] [PubMed]
25. Gardner, L.R.; Michener, W.K.; Williams, T.M.; Blood, E.R.; Kjerve, B.; Smock, L.A.; Lipscomb, D.J.; Gresham, C. Disturbance Effects of Hurricane Hugo on a Pristine Coastal Landscape: North Inlet, South Carolina, USA. *Neth. J. Sea Res.* **1992**, *30*, 249–263. [CrossRef]
26. Sklar, F.H.; Browder, J.A. Coastal Environmental Impacts Brought About by Alterations to Freshwater Flow in the Gulf of Mexico. *Environ. Manag.* **1998**, *22*, 547–562. [CrossRef]
27. Poulter, B.; Goodall, J.L.; Halpin, P.N. Applications of Network Analysis for Adaptive Management of Artificial Drainage Systems in Landscapes Vulnerable to Sea Level Rise. *J. Hydrol.* **2008**, *357*, 207–217. [CrossRef]
28. Stotts, S.; Callahan, J.; Gulledge, O. Impact of Channel Dredging and Straightening in an Atlantic White Cedar (Chamaecyparis Thyoides L. (B.S.P.)) Freshwater Tidal Wetland. *J. Coast. Res.* **2021**, *37*, 973–986. [CrossRef]
29. Krauss, K.W.; Duberstein, J.A.; Doyle, T.W.; Conner, W.H.; Day, R.H.; Inabinette, L.W.; Whitbeck, J.L. Site Condition, Structure, and Growth of Baldcypress along Tidal/Non-Tidal Salinity Gradients. *Wetlands* **2009**, *29*, 505–519. [CrossRef]
30. Martin, D.W.; Young, D.R. Small-Scale Distribution and Salinity Response of *Juniperus Virginiana* on an Atlantic Coast Barrier Island. *Can. J. Bot.* **1997**, *75*, 77–85. [CrossRef]
31. Little, E.L., Jr. *Atlas of United States Trees-Conifers and Important Hardwoods*; Miscellaneous Publication 1; United States Department of Agriculture: Washington, DC, USA, 1971.
32. Ferguson, E.R.; Lawson, E.R.; Maple, W.R.; Mesavage, C. *Managing Eastern Redcedar*; US Department of Agriculture Forest Service: New Orleans, LA, USA, 1968.
33. Burns, R.M. *Silvics of North America: Conifers*; U.S. Department of Agriculture, Forest Service: Washington, DC, USA, 1990.
34. Johnson, S.R.; Young, D.R. Factors Contributing to the Decline of Pinus Taeda on a Virginia Barrier Island. *Bull. Torrey Bot. Club* **1993**, *120*, 431–438. [CrossRef]
35. Tolliver, K.S.; Martin, D.W.; Young, D.R. Freshwater and Saltwater Flooding Response for Woody Species Common to Barrier Island Swales. *Wetlands* **1997**, *17*, 10–18. [CrossRef]
36. Harper, R.M. The Diverse Habits of the Eastern Red Cedar and Their Interpretation. *Torreya* **1912**, *12*, 145–154.
37. NOAA NCEI Climate at a Glance | National Centers for Environmental Information (NCEI). Available online: https://www.ncdc.noaa.gov/cag/ (accessed on 15 March 2022).
38. Delaware Department of Natural Resources and Environmental Control Delaware National Estuarine Research Reserve Estuarine Profile. 1999. Available online: https://coast.noaa.gov/data/docs/nerrs/Reserves_DEL_SiteProfile.pdf (accessed on 11 April 2022).
39. The Delaware Geological Survey Elevation Contours of Delaware. 2019. Available online: https://www.dgs.udel.edu/datasets/elevation-contours-delaware (accessed on 11 April 2022).
40. Ciecko, L.; Kimmett, D.; Saunders, J.; Katz, R.; Wolf, K.L.; Bazinet, O.; Richardson, J.; Brinkley, W.; Blahna, D.J. *Forest Landscape Assessment Tool (FLAT): Rapid Assessment for Land Management*; U.S. Department of Agriculture, Forest Service: Portland, OR, USA; Pacific Northwest Research Station: Portland, OR, USA, 2016; p. PNW-GTR-941.
41. Hiziroglu, S.; Zhang, D. Impact Assessment and Utilization of Eastern Redcedar. *Am. J. Appl. Sci.* **2010**, *7*, 1032–1037. [CrossRef]
42. Douglas, S. Update on the Eastern Red Cedar Problem. Available online: https://portal.ct.gov/CAES/Fact-Sheets/Plant-Pathology/Update-on-the-Eastern-Red-Cedar-Problem (accessed on 23 March 2022).
43. Gilman, E.F.; Watson, D.G. Juniperus Virginiana: Eastern Redcedar. 1993. Available online: https://edis.ifas.ufl.edu/pdf/ST/ST32700.pdf (accessed on 11 April 2022).
44. Parker, D.R. How to Take a Soil Sample for Home Lawns and Gardens. 2007. Available online: https://www.udel.edu/content/dam/udelImages/canr/pdfs/extension/environmental-stewardship/Circular-19-How-to-Take-a-Soil-Sample-for-Home-Lawns-and-Gardens.pdf (accessed on 11 April 2022).
45. Speer, J.H. *Fundamentals of Tree-Ring Research*; University of Arizona Press: Tucson, AZ, USA, 2011; ISBN 978-0-8165-2685-7.
46. Holmes, Richard Computer-Assisted Quality Control in Tree-Ring Dating and Measurement. *Tree-Ring Bull.* **1983**, *43*, 69–78.
47. Bunn, A.; Korpela, M.; Biondi, F.; Campelo, F.; Mérian, P.; Qeadan, F.; Zang, C.; Buras, A.; Cecile, J.; Mudelsee, M.; et al. DplR: Dendrochronology Program Library in R. 2021. Available online: https://cran.r-project.org/web/packages/dplR/index.html (accessed on 11 April 2022).

48. Cook, E.; Briffa, K.; Shiyatov, S.; Mazepa, V.; Jones, P.D. *Methods of Dendrochronology*; Springer: Dordrecht, The Netherlands, 1990; pp. 97–162. ISBN 978-0792305866.
49. Huntington, J.L.; Hegewisch, K.C.; Daudert, B.; Morton, C.G.; Abatzoglou, J.T.; McEvoy, D.J.; Erickson, T. Cloud Computing and Visualization of Climate and Remote Sensing Data for Advanced Natural Resource Monitoring and Process Understanding. *Bull. Am. Meteorol. Soc.* **2017**, *98*, 2397–2410. [CrossRef]
50. NOAA CO-OPS Map—NOAA Tides & Currents. Available online: https://tidesandcurrents.noaa.gov/map/index.html?region=%20NewJersey (accessed on 15 March 2022).
51. Bunn, A.; Korpela, M.; Biondi, F.; Campelo, F.; Mérian, P.; Qeadan, F.; Zang, C.; Buras, A.; Cecile, J.; Mudelsee, M.; et al. DplR: Dendrochronology Program Library in R. 2016. Available online: https://cran.r-project.org/web/packages/dplR/index.html (accessed on 11 April 2022).
52. Fritts, H.C. *Tree Rings and Climate*; Academic Press: New York, NY, USA, 1976; ISBN 978-0122684500.
53. Kratsch, H. *Boron- and Salt-Tolerant Trees and Shrubs for Northern Nevada*; UNCE Special Publication 12-04; University of Nevada, Cooperative Extention: Reno, NV, USA, 2012; Available online: https://www.fs.fed.us/rm/pubs_other/rmrs_2012_kratsch_h001.pdf (accessed on 11 April 2022).
54. Edmondson, J.R. The Meteorological Significance of False Rings in Eastern Redcedar (*Juniperus Virginiana* L.) from the Southern Great Plains, U.S.A. *Trre* **2010**, *66*, 19–33. [CrossRef]
55. Weakly, H.E. A Tree-Ring Record of Precipitation in Western Nebraska. *J. For.* **1943**, *41*, 816–819. [CrossRef]
56. Guyette, R.; McGinnes, E.A.; Probasco, G.E.; Evans, K.E. A Climate History of Boone County, Missouri, From Tree-Ring Analysis of Eastern Redcedar. *Wood Fiber Sci.* **1980**, *12*, 17–28.
57. Butler, D.; Butler, W.S.; David, R.; Walsh, S.J. The Use of Eastern Redcedar in a Tree-Ring Study in Oklahoma. *Prairie Nat.* **1988**, *20*, 47–56.
58. Copenheaver, C.A.; Kyle, K.H.; Stevens, G.N.; Kamp, M.H. Comparing *Juniperus Virginiana* Tree-Ring Chronologies from Forest Edge vs. Forest Interior Positions in the Cedars Natural Area Preserve in Virginia, USA. *Dendrochronologia* **2005**, *23*, 39–45. [CrossRef]
59. Larson, D.W. Dendroecological Potential of *Juniperus Virginiana* L. Growing on Cliffs in Western Virginia. *Banisteria* **1997**, *10*, 6.
60. Noe, G.B.; Bourg, N.A.; Krauss, K.W.; Duberstein, J.A.; Hupp, C.R. Watershed and Estuarine Controls Both Influence Plant Community and Tree Growth Changes in Tidal Freshwater Forested Wetlands along Two U.S. Mid-Atlantic Rivers. *Forests* **2021**, *12*, 1182. [CrossRef]
61. Yanosky, T.M.; Hupp, C.R.; Hackney, C.T. Chloride Concentrations in Growth Rings of Taxodium Distichum in a Saltwater-Intruded Estuary. *Ecol. Appl.* **1995**, *5*, 785–792. [CrossRef]
62. Thomas, B.L.; Doyle, T.; Krauss, K. Annual Growth Patterns of Baldcypress (Taxodium Distichum) Along Salinity Gradients. *Wetlands* **2015**, *35*, 831–839. [CrossRef]
63. Rheinhardt, R.D. Tidal Freshwater Swamps of a Lower Chesapeake Bay Subestuary. In *Ecology of Tidal Freshwater Forested Wetlands of the Southeastern United States*; Conner, W.H., Doyle, T.W., Krauss, K.W., Eds.; Springer: Dordrecht, The Netherlands, 2007; pp. 161–182. ISBN 978-1-4020-5095-4.
64. Anderson, C.J.; Lockaby, B.G. Foliar Nutrient Dynamics in Tidal and Non-Tidal Freshwater Forested Wetlands. *Aquat. Bot.* **2011**, *95*, 153–160. [CrossRef]
65. Noe, G.B.; Krauss, K.W.; Lockaby, B.G.; Conner, W.H.; Hupp, C.R. The Effect of Increasing Salinity and Forest Mortality on Soil Nitrogen and Phosphorus Mineralization in Tidal Freshwater Forested Wetlands. *Biogeochemistry* **2013**, *114*, 225–244. [CrossRef]
66. Weston, N.B.; Dixon, R.E.; Joye, S.B. Ramifications of Increased Salinity in Tidal Freshwater Sediments: Geochemistry and Microbial Pathways of Organic Matter Mineralization. *J. Geophys. Res. Biogeosci.* **2006**, *111*, 1–14. [CrossRef]